THE UNIVERSITY *of* EDINBURGH

Edinburgh Research Explorer

Kindlin-1 promotes pulmonary breast cancer metastasis

OPEN ACCESS

Kindlin-1 promotes pulmonary breast cancer metastasis

Sana Sarvi[1*], Hitesh Patel[1*†], Jun Li[1], Georgia L. Dodd[1], Helen Creedon[1], Morwenna Muir[1], Jocelyn Ward[1‡], John C. Dawson[1], Martin Lee[1], Jayne Culley[1], Donald M. Salter[2], Andrew H. Sims[1], Adam Byron[1], Valerie G. Brunton[1]

[1]Cancer Research UK Edinburgh Centre and [2]Centre for Genomic & Experimental Medicine, Institute of Genetics and Molecular Medicine, University of Edinburgh, Edinburgh EH4 2XR, United Kingdom

[†]Current address: Sussex Drug Discovery Centre, School of Life Sciences, University of Sussex, Brighton BN1 9QJ, United Kingdom

[‡]Current address: Magdalen College, University of Oxford, Oxford OX1 4AU, United Kingdom

[*]These authors contributed equally to the work

Correspondence: Valerie G. Brunton

Cancer Research UK Edinburgh Centre, Institute of Genetics and Molecular Medicine, University of Edinburgh, Crewe Road South, Edinburgh EH4 2XR, United Kingdom

email: v.brunton@ed.ac.uk

tel.: +44 (0)131 651 8500; fax: +44 (0)131 651 8800

Running title: Kindlin-1 regulates mammary tumor metastasis

Key words: Kindlin-1, adhesion, metastasis

The authors declare no conflicts of interest.

Abstract

In breast cancer, increased expression of the cytoskeletal adaptor protein Kindlin-1 has been linked to increased risks of lung metastasis, but the functional basis is unknown. Here we show that in a mouse model of polyomavirus middle T antigen-induced mammary tumorigenesis, loss of Kindlin-1 reduced early pulmonary arrest and later development of lung metastasis. This phenotype relied on the ability of Kindlin-1 to bind and activate β integrin heterodimers. Kindlin-1 loss reduced α4 integrin-mediated adhesion of mammary tumor cells to the adhesion molecule VCAM-1 on endothelial cells. Treating mice with an anti-VCAM-1 blocking antibody prevented early pulmonary arrest. Kindlin-1 loss also resulted in reduced secretion of several factors linked to metastatic spread, including the lung metastasis regulator tenascin-C, showing that Kindlin-1 regulated metastatic dissemination by an additional mechanism in the tumor microenvironment. Overall, our results show that Kindlin-1 contributes functionally to early pulmonary metastasis of breast cancer.

Statement of significance

Findings provide a mechanistic proof in mice that Kindin-1, an integrin-binding adaptor protein, is a critical mediator of early lung metastasis of breast cancer.

3

INTRODUCTION

Metastasis is the spread of cancer cells from a primary tumor to distant sites within the body to establish secondary tumors or metastases. Although this is a highly inefficient process, the consequences are devastating as metastatic disease accounts for more than 90% of cancer-related mortality. Recent work in breast cancer identified *FERMT1* in a six-gene signature that can classify breast tumors with a higher propensity to metastasize to the lungs, independent of the molecular subtype [1, 2]. Subsequent analysis showed that *FERMT1* expression was associated specifically with lung metastasis-free survival in breast cancer [3]. *FERMT1* encodes Kindlin-1, which is a four-point-one, ezrin, radixin, moesin (FERM) domain-containing protein that is localized at focal adhesion sites, where it interacts with the β-subunit of integrins and regulates their activity [4]. It was first identified as a gene whose loss or mutation is linked to Kindler syndrome (KS), which is an autosomal recessive disease that leads to skin abnormalities including blistering, atrophy, photosensitivity and poikiloderma [5]. Some of these phenotypes have been attributed to defects in β1 integrin activation in keratinocytes from KS patients [6], and in addition, deletion of *Fermt1* in the mouse skin leads to skin defects that recapitulate some aspects of KS that have been linked to a disruption of integrin activation [7]. However, other studies have shown that Kindlin-1 has additional integrin-independent cellular roles [7-9].

The molecular mechanisms whereby Kindlin-1 specifically regulates metastasis to the lung in breast tumors are largely unknown. Initial studies have shown that Kindlin-1 regulates TGFβ-induced epithelial-to-mesenchymal transition (EMT) in breast cancer cell lines, which has been attributed to an increased invasive capacity [3]. To investigate further the role of Kindlin-1 in metastasis and understand how it

4

may impact on the different steps of the metastasis cascade, we have used the polyomavirus middle T (PyV MT)-driven mouse model of mammary tumorigenesis that metastasizes to the lungs. In this model, specific deletion of Kindlin-1 in the mammary epithelium significantly delayed tumor onset and reduced lung metastasis. We show that Kindlin-1 expression is essential for lung metastasis and enhances the metastatic potential of breast cancer cells by specifically modulating integrin activity and promoting tumor cell adhesion at the metastatic niche while also regulating the secretion of a number of metastasis-associated proteins.

MATERIALS AND METHODS

Animals. Kin-1$^{fl/fl}$ mice were generated by Taconic Biosciences. MMTV-Cre [10], MMTV-PyV MT [11] and MMTV-NIC [12] mice were from W.J. Muller (McGill University, Montreal, Quebec, Canada), and ROSA26-tdRFP [13] mice were from O.J. Sansom (Cancer Research UK Beatson Institute, Glasgow, UK). All transgenic mice were derived from the inbred FVB/N strain. Mice were monitored weekly for tumor formation by palpation (tumor onset was defined as presence of a palpable tumor). Animals were sacrificed once their tumor burden had reached the maximum size, as determined by UK Home Office regulations. Tumors and tissues were removed and fixed in 10% buffered formalin at sacrifice and subsequently paraffin embedded. All animal experiments were approved by the University of Edinburgh Animal Welfare and Ethical Review Body (approval PL01-16) and the UK Home Office (PPL 70/8897).

Cell lines. Met-1 cells were from B. Qian (University of Edinburgh) and have been described previously [14] and were authenticated using CellCheck^{TM} (IDEXX). Cells were mycoplasma tested every month and were used within three months of recovery

5

from frozen. Two 19-base-pair oligos (TGTCTGGGGACCTACATAT (A) and TTTTCGGCTGTGGTGTTTA (B)) corresponding to homologous regions near the start methionine of Kindlin-1 and adjacent to protospacer adjacent motif (NGG) sites were selected as guide RNAs (gRNAs) using the Blue Heron gRNA target design tool (https://wwws.blueheronbio.com/external/tools/gRNASrc.jsp). Fragments A and B were cloned into a gRNA expression vector (plasmid #41824; Adgene/Church Lab), and together with a Cas9 expression vector (plasmid #41815; Adgene/Church Lab), were transfected (Lipofectamine 2000; Thermo Fisher Scientific) into Met-1 cells.

Experimental metastasis assay. Tumors were digested in 2 mg/ml collagenase D and 100 unit/ml hyaluronidase (Worthington) in serum-free DMEM for 1 hour. Single cell suspensions were injected into the tail vein of recipient mice (4 mice per tumor and 5 tumors per genotype). Eight weeks after injection, animals were sacrificed, lungs collected, weighed and fixed in 10% buffered formalin for subsequent H&E staining. Further quantification was carried out using q-PCR with primers against the PyV MT transgene, as described previously [15]. For treatment with VCAM-1 blocking antibody, mice were injected with 7 mg/kg anti-VCAM-1 antibody (clone M/K-2.7; Bio X Cell) [16] or its corresponding IgG1 isotype control (clone HRPN; Bio X Cell) 4 hours prior to injecting cells. For treatment with α4 integrin blocking antibody, cells were incubated with 1.5 mg/ml anti-α4-integrin antibody (clone PS/2; Bio X Cell) or isotype control 30 minutes prior to injection.

Flow cytometry. Samples were stained with APC-conjugated anti-β1 integrin (1:100; eBioscience), anti-β1 integrin (clone 9EG7, 5 μg/ml; BD Biosciences) or Alexa Fluor 488-conjugated anti-VCAM-1 (10 μg/ml; AbD Serotec) antibodies and the viability dye eFluor 506 (1:200; eBioscience). Alexa Fluor 647-conjugated anti-rat IgG (1:200;

6

eBioscience) secondary antibody was used for 9EG7 staining. Samples were processed on a FACSAria (BD Biosciences) and data analyzed using FlowJo software (TreeStar).

Western blotting. Cell lysates were resolved by gel electrophoresis, transferred to nitrocellulose, and probed with anti-Kindlin-1 (1:3000; Abcam), anti-His-tag (D3I1O, 1:1000; Cell Signaling Technology) or anti-actin (1:5000; Cell Signaling Technology) antibodies, followed by goat anti-mouse or goat anti-rabbit IRDye 680- or 800-labeled secondary antibodies (LI-COR Biosciences). Membranes were imaged using an Odyssey infrared scanner (LI-COR Biosciences).

Immunohistochemistry. Formalin-fixed tissue samples were incubated with anti-RFP (1:100; Rockland Immunochemicals) or anti-Ki67 (1:800; Vector Laboratories) antibodies, followed by HRP-conjugated secondary antibodies (Jackson ImmunoResearch Laboratories). Slides were counterstained with Mayer's hematoxylin.

Cell attachment assay. Fibronectin (10 μg/ml, Corning) or VCAM-1 (10 μg/ml, R&D Systems) coated wells were blocked with 10 mg/ml heat-denatured BSA for 30 minutes. For adhesion to fibronectin, cells were allowed to attach for 10 minutes at 37°C. Adherent cells were fixed with 5% glutaraldehyde and stained with 0.1% crystal violet solution. The dye was solubilized in 10% acetic acid, and absorbance measured at 570 nm. For adhesion to VCAM-1, cells were incubated with Hoechst 33342 (5 μg/ml; Thermo Fisher Scientific) for 10 minutes before plating on VCAM-1-coated wells for 30 minutes at 37°C. Adherent cells were imaged and analyzed using an ImageXpress high-content analysis system (Molecular Devices). For antibody blocking experiments, cells were incubated with anti-α4 integrin antibody

7

(clone PS/2, 10 μg/ml; Abcam) for 1 hour at room temperature before attachment to VCAM-1.

Tumor cell–endothelial cell binding assay. 3B-11 mouse endothelial cells (ATCC) were plated in 24-well plates and incubated for 48 hours to obtain a uniform monolayer. Cells were mycoplasma tested every month and were used within two months of recovery from frozen. Cells were purchased from ATCC and no further authentication was carried out. Tumor cells were labeled with Hoechst 33342 (5 μg/ml) for 10 minutes at 37°C before adhesion to the endothelial cell monolayer for 10 minutes at 37°C. Wells were washed twice with PBS and images acquired on an ImageXpress high-content analysis system. For antibody blocking experiments, cells were treated with either anti-α4 integrin antibody (clone PS/2, 10 μg/ml) or anti-VCAM-1 antibody (clone M/K-2.7, 10 μg/ml) for 1 hour before attachment to the endothelial cells.

Secretome isolation and preparation. Conditioned medium was collected in serum-free, phenol-red-free DMEM for 48 hours, clarified of cellular debris by centrifugation, filtered through a 0.22-μm filter and concentrated at 4°C using a 9k MWCO Pierce protein concentrator (Thermo Fisher Scientific). Proteins were precipitated using trichloroacetic acid/acetone and resolubilized in 8 M urea, 100 mM ammonium bicarbonate, 10 mM dithiothreitol for 30 minutes at 37°C. Proteins were alkylated using 25 mM iodoacetamide for 30 minutes at room temperature in the dark, after which excess iodoacetamide was quenched using 5 mM dithiothreitol, and then urea concentration was diluted to 2 M using 100 mM ammonium bicarbonate. Samples were incubated with PNGase F for 2 hours at 37°C, then 1:100 (w:w, enzyme:protein) Lys-C for 2 hours at 37°C, then 1:50 trypsin for 16 hours at 37°C,

8

then 1:100 trypsin for 2 hours at 37°C. Resultant peptides were acidified to a final concentration of 0.5% trifluoroacetic acid, and 10 μg were desalted using C18 StageTips.

Label-free mass spectrometry (MS) and bioinformatic analyses. Liquid chromatography–MS was performed using an UltiMate 3000 RSLCnano system (Thermo Fisher Scientific) coupled online to a Q Exactive Plus mass spectrometer (Thermo Fisher Scientific). MS data were searched against the mouse UniProtKB database (version September 2015) using MaxQuant (version 1.5.3.17) (peptide and protein false discovery rates (FDRs), 1%) and further analyzed using Perseus (version 1.5.2.6). Instrument settings and data analysis parameters are detailed in the Supplementary data file. Association networks were analyzed using Cytoscape (version 3.3.0). Extracellular protein annotations were extracted from the Gene Ontology Slim database, reported associations with metastasis were extracted from the Molecular Signatures Database (version 6.0) and manual literature curation, and integrin ligand designations were extracted from work by Humphries *et al.* [17] and manual literature curation. Gene expression analysis across a compendium of 2999 breast tumors from 17 Affymetrix datasets was performed as described previously [18]. *FERMT1* status was determined by 'present' detection calls using the MAS5 algorithm [19]. Cox proportional hazards survival analysis was performed for all possible points-of-separation (low–high cut-points) for each gene [20].

RESULTS

Loss of Kindlin-1 delays mammary tumor onset but not growth of established tumors

9

To evaluate whether loss of Kindlin-1 altered mammary tumor development, we generated mice in which exons 4 and 5 of the *Fermt1* gene were flanked with LoxP1 recombination sites. Excision of the *Fermt1* gene in the mammary epithelium was achieved by crossing with mice in which Cre recombinase was expressed in the mammary epithelium under transcriptional control of the mouse mammary tumor virus (MMTV-Cre) [10] to generate MMTV-Cre/Kin-1$^{fl/fl}$ mice. Recombination of the *Fermt1* allele in the mammary epithelium was confirmed at the DNA level (Supplementary Fig. S1A), which was accompanied by reduced protein expression in the isolated mammary epithelial cells (Supplementary Fig. S1B and C). Kindlin-1 was localized within the ducts, where it co-localized with β1 integrin, and this expression was reduced in the MMTV-Cre/Kin-1$^{fl/fl}$ mice (Supplementary Fig. S1D). Complete loss of Kindlin-1 expression in the mammary epithelium was not seen, which most likely reflects the stochastic nature of the MMTV-Cre expression [21]. This was confirmed by crossing the MMTV-Cre mice with mice carrying a Cre-responsive ROSA26-tdRFP reporter (ROSA-tdRFP) [13]. Staining of mammary glands from the resulting offspring showed expression of the Cre transgene in around 60% of the mammary ducts (Supplementary Fig. S1E). The percentage of recombination was not significantly altered in the MMTV-Cre/Kin-1$^{fl/fl}$ mice, indicating that there was no preferential retention or selective advantage for the Kindlin-1-positive cells in the developing mammary gland.

MMTV-Cre/Kin-1$^{fl/fl}$ animals were then bred with mice carrying the PyV MT transgene under transcriptional control of the mouse mammary tumor virus (MMTV-PyV MT) [11]. Cohorts of MMTV-PyV MT-Kin-1$^{wt/wt}$ (MT-Kin-1$^{wt/wt}$) and MMTV-PyV MT-Kin-1$^{fl/fl}$ (MT-Kin-1$^{fl/fl}$) mice were aged, and mammary tumor development monitored. Ablation of Kindlin-1 in mouse mammary epithelium significantly

10

delayed tumor onset, with a median onset of 70 days in the MT-Kin-1$^{fl/fl}$ animals and 32.5 days in the MT-Kin-1$^{wt/wt}$ animals (Fig. 1A). Analysis of fat pads from 28-day-old mice showed that 57% of the fat pad was covered by focal lesions in MT-Kin-1$^{wt/wt}$ mice, with only 13% of the area covered in MT-Kin-1$^{fl/fl}$ mice (Fig. 1B and C). Whole mount analysis of mammary glands from 4-, 6-, and 12-week-old female virgin Kin-1$^{fl/fl}$ and Kin-1$^{wt/wt}$ mice showed that there was no effect of Kindlin-1 loss on normal mammary gland development, with no significant difference in the ductal network area between the groups at each time point (4 weeks, $P = 0.232$; 6 weeks, $P = 0.459$; 12 weeks, $P = 0.431$) (Supplementary Fig. S1F). H&E staining did not reveal any difference in duct morphology (Supplementary Fig. S1G).

To confirm the effects on tumor onset, we utilized the MMTV-NIC (Neu-IRES-Cre) model of mammary tumor development [12], which employs a bicistronic transcript to co-express activated ErbB2/Neu with MMTV-Cre recombinase, resulting in the formation of activated ErbB2/Neu-driven mammary tumors. There was a significant delay in tumor onset in NIC-Kin-1$^{fl/fl}$ mice (Supplementary Fig. S2A) (median onset, NIC-Kin-1$^{wt/wt}$, 113 days; NIC-Kin-1$^{fl/fl}$, 152 days).

The difference in tumor initiation was mirrored by an increased survival in both the MT-Kin-1$^{fl/fl}$ and NIC-Kin-1$^{fl/fl}$ mice (Supplementary Fig. S2B and C) as there was no difference in the tumor doubling times of established tumors between the two mouse genotypes (Fig. 1D). Reduced Kindlin-1 expression in the tumors was confirmed by western blot (Supplementary Fig. S2D), while immunohistochemical analysis of Ki67 expression in size-matched tumors taken from MT-Kin-1$^{wt/wt}$ and MT-Kin-1$^{fl/fl}$ animals confirmed a similar proliferation rate between the two groups (Fig. 1E). Histologically, the tumors in both the MT-Kin-1$^{wt/wt}$ and MT-Kin-1$^{fl/fl}$ mice were similar, showing mixed papillary, acinar and solid growth patterns (Fig. 1F).

11

Kindlin-1 loss reduces pulmonary metastasis

To assess the importance of Kindlin-1 loss in metastatic spread, we analyzed lungs from both MT-Kin-1$^{wt/wt}$ and MT-Kin-1$^{fl/fl}$ mice. There was a reduction in the number of mice with metastatic lesions in the MT-Kin-1$^{fl/fl}$ mice (Fig. 2A and B). Furthermore, MT-Kin-1$^{wt/wt}$ mice demonstrated a 27-fold higher metastatic burden than MT-Kin-1$^{fl/fl}$ mice when normalized to the total primary tumor weight, as analyzed by q-PCR of the tumor-specific PyV MT in the lungs (Fig. 2C).

To establish whether the decreased pulmonary metastasis seen in the MT-Kin-1$^{fl/fl}$ mice was a result of impaired lung colonization, dissociated cells from tumors taken from either MT-Kin-1$^{fl/fl}$ or MT-Kin-1$^{wt/wt}$ mice were injected into the tail vein of recipient wild-type mice, and metastasis quantified 8 weeks post-injection. Reduced Kindlin-1 expression in the MT-Kin-1$^{fl/fl}$ tumor cells prior to injection was confirmed by western blot (Supplementary Fig. S2E). There was a significant reduction in metastatic burden when Kindlin-1-depleted cells were injected, as measured by lung weight (Fig. 2D) and area covered by metastatic lesions (Fig. 2E). Further analysis showed that the number of metastatic lesions was reduced following injection of the Kindlin-1-depleted cells, although this did not reach statistical significance (Fig. 2F). The metastases that did form were significantly smaller than those seen upon injection of the Kindlin-1-expressing cells (Fig. 2G) and this was accompanied by a small but non-significant reduction in Ki67 staining (Fig. 2H). Thus, Kindlin-1 can influence metastatic colonization: the small changes seen in some of the outputs may reflect the variability in Kindlin-1 depletion in the primary tumor cells that were injected (Supplementary Fig. S2E) and therefore further studies to determine the role of Kindlin-1 were carried out in the Met-1 cell line in which the *Fermt1* gene was deleted as detailed below.

12

Kindlin-1 regulates integrin activity in mammary tumors

As Kindlin-1 is a known regulator of integrin activation, we asked whether loss of Kindlin-1 affects integrin activation in the mammary tumors. Integrin activation state was assessed by flow cytometry using the 9EG7 antibody, which recognizes an active-specific epitope on β1 integrin [22]. Tumors from MT-Kin-1^{wt/wt} mice exhibited significantly higher levels of active cell-surface β1 integrin compared to tumors from MT-Kin-1^{fl/fl} mice, with no difference in total cell-surface β1 integrin expression (Fig. 3A and B and Supplementary Fig. S2F).

To investigate further the role of Kindlin-1 and integrin activation in pulmonary metastasis, we used the Met-1 cell line, which is derived from an MMTV-PyV MT mammary tumor [14]. Using the CRISPR-Cas9 system with two different guide RNAs (gRNA-A and -B), the *Fermt1* gene was deleted in the Met-1 cells. Single-cell clones were isolated from the two different gRNA transfections in which Kindlin-1 deletion was targeted. The loss of Kindlin-1 was confirmed at both the transcript and the protein level (Supplementary Fig. S3A and B). To assess whether the effects of Kindlin-1 loss on metastasis were dependent on its ability to regulate integrin activity, we re-introduced either wild-type Kindlin-1 (WT) or a Kindlin-1 mutant that is unable to bind and activate β integrin tails (AA) [23, 24] into the Kindlin-1 knock-out (Null) cells to levels similar to the endogenous Kindlin-1 found in the parental Met-1 cells (Supplementary Fig. S3C). Ectopic expression of wild-type Kindlin-1 and Kindlin-1-AA into the null clones derived from both gRNA-A and gRNA-B was carried out in a number of different clones (Fig. 3C, gRNA-A clone A1 (A1), and Supplementary Fig. S3D). In WT cells (null cells in which wild-type Kindlin-1 has been ectopically expressed), the presence of Kindlin-1 was associated with higher β1 integrin activity compared to Null cells (Fig. 3D and Supplementary Fig. S4A–C). Moreover, AA cells

13

(null cells in which the Kindlin-1 AA mutant has been ectopically expressed) exhibited levels of β1 integrin activity similar to those of Null cells, confirming the importance of Kindlin-1 in regulating integrin activation in the PyV MT-derived mammary tumor cells. Consistent with the reduced β1 integrin activation, attachment to fibronectin was significantly reduced in the Null cells, and this was not restored in the AA cells (Fig. 3E and Supplementary Fig. S4D).

Kindlin-1-dependent integrin activation is required for the early stages of lung colonization

To address whether Kindlin-1 regulation of integrin activation was required for metastatic colonization in the lungs, we injected Null, WT and AA cells into the tail vein of mice and analyzed metastatic burden after 21 days. Animals receiving WT cells had significantly higher levels of metastasis compared to animals receiving Null cells. Re-expression of Kindlin-1-AA did not restore the metastatic capacity of the Null cells (Fig. 3F and Supplementary Fig. S4E).

As we had seen a reduced number of metastatic lesions in the lungs following injection of disseminated tumor cells from the MT-Kin-1$^{fl/fl}$ mice (Fig. 2F), we asked whether Kindlin-1 plays a role in very early metastatic colonization. Cells were injected into the tail vein, and the lungs removed 30 minutes post-injection, a time when adhesion of tumor cells in the lung has been shown to be important for subsequent metastatic outgrowth [25, 26]. There was a significant reduction in tumor cell accumulation in the lungs of animals injected with Null cells compared to WT cells, and this was not restored upon injection of the AA cells (Fig. 3G and Supplementary Fig. S4F). These data indicate that Kindlin-1 enables pulmonary colonization at early stages of metastasis, which is dependent on integrin activation.

14

Kindlin-1 loss inhibits tumor cell attachment to endothelial cells

At very early stages of lung colonization, tumor cell attachment to endothelial cells and their subsequent transendothelial migration occurs [24]. Tumor cells are known to bind to vascular cell adhesion molecule-1 (VCAM-1) expressed on endothelial cells via α4β1 integrin [27]. Loss of Kindlin-1 reduced adhesion of the Met-1 cells to recombinant VCAM-1 compared to Kindlin-1-expressing cells, and this was not rescued by expression of Kindlin-1-AA (Fig. 4A and Supplementary Fig. S5A and B). Treatment with an anti-α4 integrin blocking antibody reduced adhesion of the WT cells to VCAM-1 to levels comparable with the Null and AA cells, while having no effect on the adhesion of the Null and AA cell lines (Fig. 4A and Supplementary Fig. S5A and B), confirming a α4 integrin-dependent mechanism. Loss of Kindlin-1 also reduced adhesion to endothelial cells, which was not restored to levels seen in WT cells by expression of the integrin-binding AA mutant (Fig. 4B and Supplementary Fig. S5C and D). Treatment with the anti-α4 integrin blocking antibody significantly reduced endothelial cell adhesion of the WT cells to levels seen in the Null and AA cells, while there was no effect on adhesion of the Null and AA cells (Fig. 4B). To determine whether adhesion of the Met-1 cells to the endothelial cells was mediated via VCAM-1, we used an anti-VCAM-1 blocking antibody, which reduced adhesion of the WT cells to the endothelial cells (Fig. 4C and Supplementary Fig. S5C and D). The tumor cells expressed very low levels of VCAM-1 compared to the endothelial cells (Supplementary Fig. S5E and F), and taken together with the inability of the anti-VCAM-1 blocking antibody to reduce the adhesion of the Null and AA cells, in which integrin activation is impaired (Fig. 4C and Supplementary Fig. S5C and D), supports a mechanism by which adhesion of the tumor cells to endothelial cells is

15

mediated via tumor-expressed α4 integrin and VCAM-1 expressed on the endothelial cells.

Finally, treatment with either an anti-VCAM-1 or α4-integrin blocking antibody prior to tumor cell injection reduced lung colonization of the WT cells, confirming the regulation of early pulmonary colonization by integrin-dependent adhesion (Fig. 4D and E). To determine whether the reduced adhesion of the Null cells could promote increased cell death leading to reduced colonization, we carried out an anoikis experiment. Loss of adhesion resulted in a 20% reduction in cell viability, but there was no difference in cell death between the WT, Null and AA cells (Supplementary Fig. S5G). This supports a mechanism whereby Kindlin-1 regulates the mechanical adhesion and trapping of cells within the lung vasculature required for lung colonization.

Proteomic analysis identifies Kindlin-1-dependent expression of metastasis regulators

Owing to the significant defect in early tumor cell arrest in the Null cells within the lung, it was not possible to address the additional impact of Kindlin-1 on the outgrowth of the disseminated cells that we had observed following injection of the disseminated MT-Kin-1$^{fl/fl}$ tumor cells (Fig. 2F–H). Therefore, to address whether Kindlin-1 may have additional roles in the metastatic cascade, we undertook label-free quantitative MS analysis of secreted factors using the WT and Null Met-1 cells, as tumor-secreted proteins are known to play an important role in regulating metastatic spread [28]. The proteomic dataset was significantly enriched for extracellular proteins (Fig. 5A); 944 extracellular proteins were quantified in at least two of the three biological replicate experiments. Protein quantification was highly

16

reproducible between biological replicate experiments ($r \geq 0.94$; $P < 0.0001$), with cell-type-specific profiles of extracellular protein levels determined by hierarchical clustering and principal component analyses (Fig. 5B and Supplementary Fig. S6A), indicating that Kindlin-1 expression affects the composition of the Met-1 secretome.

Expression of more than two-thirds of the proteins in the Kindlin-1-dependent secretome (67.5%) has been reported to correlate with metastasis in other studies, including both metastasis suppressors and promoters (Fig. 5B and Supplementary Table S1). Consistent with the reported association of Kindlin-1 with EMT in breast cancer cell lines [3], the Kindlin-1-dependent secretome was also significantly enriched for proteins associated with EMT (Supplementary Fig. S6B). In addition to anticipated extracellular matrix and adhesion molecule binding functions, serine protease inhibitor activity was significantly overrepresented in the Kindlin-1-dependent secretome (Fig. 5C). Tenascin-C was the most enriched (88-fold) secreted protein following re-expression of Kindlin-1 in the Null cells (Fig. 5D). Tenascin-C is a large glycoprotein that binds a number of membrane receptors and extracellular matrix proteins, and its expression is associated with poor metastasis-free and overall survival in breast cancer patients [29]. The second secreted protein most substantially enriched in a Kindlin-1-dependent manner (21-fold) was plasminogen activator inhibitor 1 (PAI-1; encoded by *Serpine1*). PAI-1 is a serine protease inhibitor with roles in integrin-mediated cell migration, extracellular matrix degradation and blood clotting (Fig. 5D), and its expression correlates with disease-free survival and overall survival in human breast cancer [30, 31]. To understand the functional context within which the dysregulated secreted proteins may interact, we constructed a composite functional association network of the Kindlin-1-dependent secretome, integrating multiple association data sources. Topological analysis of the secretome network

17

revealed tenascin-C and PAI-1 linked to highly interconnected protein neighbors in the network, suggesting that they may connect or participate in subnetworks of extracellular proteins that may be functionally related (Fig. 5E, Supplementary Fig. S6C–E and Supplementary Table S1). Analysis of the inferred neighbors of tenascin-C and PAI-1 in the Kindlin-1-dependent secretome network revealed that the majority (88.6%) have been linked to metastasis and several are extracellular integrin ligands (5 enriched upon loss of Kindlin-1; 8 enriched upon Kindlin-1 re-expression) (Fig. 5F). These data implicate this putative subnetwork of secreted proteins in an additional, microenvironmental level of Kindlin-1-dependent regulation of metastatic dissemination.

Analysis of *Tnc* and *Serpine1* by q-RT-PCR in the Met-1 cell lines showed that the decreased secretion of tenascin-C following Kindlin-1 loss (Fig. 5D and F) was mirrored by a loss of *Tnc* transcript, while *Serpine1* transcript levels were unaltered (Fig. 6A). Furthermore, expression of the Kindlin-1 AA mutant that is unable to bind and activate β integrin tails also resulted in a loss of *Tnc* transcript, indicating that *Tnc* expression is dependent on Kindlin-1-mediated integrin activity. As tenascin-C is required for the outgrowth of pulmonary micrometastases [32], we asked whether the outgrowth of micrometastases was also dependent on integrin activity. We generated an A1 WT cell line that expresses β1 integrin shRNA under the conditional control of doxycycline (Supplementary Fig. S6F) and carried out an experimental metastasis assay. Following tail vein injection of the cells, they were allowed to reside in the lungs for 7 days before treatment with doxycycline to suppress β1 integrin expression. The metastatic burden was analyzed after a further 14 days and showed a significant reduction in the doxycycline-treated animals (Supplementary Fig. S6G),

18

demonstrating that β1 integrin is required for the outgrowth of the disseminated tumor cells.

The Kindlin-1-dependent secretome is associated with lung metastasis

TNC expression in pulmonary metastatic lesions has previously been shown to be associated with poor overall survival of patients with breast cancer [32]. Analysis of the lung metastasis signature generated in the human MDA-MB-231 breast cancer model [33] showed a strong correlation between *FERMT1* and the lung metastatic capacity of MDA-MB-231 variants, as seen with *TNC* (Fig. 6B and C). In contrast, there was no positive correlation between *SERPINE1* and lung metastatic capacity (Fig. 6B and C). Similarly, analysis of *TNC*, *FERMT1* and *SERPINE1* across a compendium of 2999 primary human breast tumors confirmed a positive correlation between high *FERMT1* expression and *TNC,* but not *SERPINE1* (Fig. 6D). Gene set enrichment analysis demonstrated that mRNA levels of the 89 Kindlin-1-dependent secretome genes represented in a published cohort of 82 primary breast cancer tumors (MSK82, GSE2603) [34] were associated with lung metastasis ($P = 0.007$). To comprehensively assess the prognostic value of the Kindlin-1-dependent secretome, we used an exhaustive survival analysis approach [20], stratifying the cohort at all possible cut-points for each secretome gene, which enabled us to quantify the association of the genes with lung or other (non-lung) metastasis. Cox proportional hazards survival analysis of each of the genes demonstrated that more of them had a greater proportion of cut-points associated with lung metastasis than non-lung metastasis ($P = 4 \times 10^{-5}$) (Fig. 6E). The significantly increased association of the secretome genes with lung metastasis was confirmed in a larger breast cancer cohort (GSE12276; $n = 204$, $P = 2 \times 10^{-9}$), although association in an overall better

19

prognosis, lymph-node-negative patient dataset did not reach statistical significance (GSE2034; $n = 286$, $P = 0.23$) (Supplementary Fig. S6H). These data suggest that the Kindlin-1-dependent secretome genes are more associated with worse outcomes in terms of lung metastasis as compared to non-lung metastasis.

DISCUSSION

Here, we provide the first direct evidence that loss of Kindlin-1 results in reduced metastatic spread using a mouse mammary tumor model. Our proteomic analysis of the Kindlin-1-dependent secretome, demonstrating significant alterations in the secretion of a number of metastasis-associated proteins, further supports a key role for Kindlin-1 in defining the metastatic potential of tumor cells. It is becoming increasingly evident that tumor cell-secreted factors can impact on the metastatic niche, thereby providing a more permissive environment for tumor cell colonization. For example, tenascin-C promotes metastatic colonization of breast cancer cells within the lung by supporting the viability of disseminated cells through activation of Notch and Wnt signaling pathways [32]. Given the correlation between *FERMT1* and *TNC* in breast cancer tissues, it will be important to establish how Kindlin-1 regulates *TNC* expression and the secretion of tenascin-C and whether this impacts on the metastatic niche. Clinical data have highlighted increased expression of Kindlin-1 associated with pulmonary metastatic spread [3], and analysis of breast cancer gene expression datasets demonstrated significantly greater associations of genes representing the Kindlin-1-dependent secretome with lung than non-lung sites of metastasis. Further studies on whether Kindlin-1 preferentially promotes pulmonary metastases and how this is linked to the Kindlin-1-dependent secretome are required.

In addition to regulation of metastasis-associated secreted proteins, we have

20

identified a role for Kindlin-1 in the very early stages of mammary tumor cell arrest in the lung vasculature. Significant effects on lung colonization upon loss of Kindlin-1 were seen as early as 30 minutes after injection of the tumor cells into the circulation. At this time, cells have arrested in the lung, but no extensive extravasation is seen [15]. In addition, recruitment of other host cells, such as macrophages and platelets, which are known to promote metastatic colonization, does not occur at this early stage of tumor cell arrest [15, 34, 35]. However, early α3β1 integrin-mediated tumor cell attachment to laminin-5 at exposed areas of the basement membrane in the lung vasculature has been reported [26]. Taken together with our data showing that the reduced metastatic dissemination of Kindlin-1-deficient cells is dependent on integrin binding and activation, this is consistent with early pulmonary arrest being an integrin-dependent event and not just due to size restriction of the tumor cells in the vascular bed. Specifically, we have identified a role for Kindlin-1 in regulating the α4 integrin-dependent adhesion of tumor cells to endothelial cells via VCAM-1. Metastatic potential correlates with expression of α4 integrin (also known as VLA-4) in various cell lines [36, 37], and α4β1 integrin has been shown to be important for attachment of tumor cells to endothelial VCAM-1 [27, 38], transendothelial migration in vitro [39, 40] and metastasis in experimental metastasis models [38, 41, 42]. Thus, Kindlin-1 may facilitate metastasis by promoting α4β1 integrin-mediated adhesion of tumor cells to endothelial cells at the early stages of disseminated tumor cell arrest in the metastatic niche. Interestingly, in a previous study, use of an anti-VCAM-1 blocking antibody showed that VCAM-1 was important for the TNFα-mediated enhancement of lung colonization, but had no effect on basal tumor cell colonization, suggesting that VCAM-1 was only important in the later stages associated with endothelial cell activation and myeloid cell recruitment [41]. However, we have also

21

identified a role for VCAM-1 in the early stages of tumor cell arrest in the pulmonary vasculature, and this may reflect the distinct repertoire of integrins expressed in different tumor cells that are able to bind to VCAM-1.

Several studies have shown that metastatic spread is regulated by β1 integrin [43-46]. In some studies, effects at later stages of lung colonization have been observed whereby loss of integrin activation in tumor cells is associated with reduced adhesion-dependent signaling to pathways such as Src and focal adhesion kinase [44, 45] and re-organization of the actin cytoskeleton, which is required for the subsequent survival and outgrowth of tumor cells in the metastatic niche [47, 48]. Taken together with our direct demonstration that β1 integrin is required for the outgrowth of disseminated tumor cells, it will be important to establish whether Kindlin-1 loss also impacts on these later aspects of lung colonization following extravasation of the tumor cells. This could be mediated via regulation of integrin signaling and adhesion to extracellular matrix components such as fibronectin, which is impaired in the Kindlin-1-depleted cells. Moreover, the finding that Kindlin-1 can regulate the secretion of a number of key metastasis-associated proteins indicates that Kindlin-1 may have wider functions in controlling the metastatic potential of tumor cells. Further mechanistic studies are required to determine the significance of the Kindlin-1 dependent secretome on metastatic spread and whether they are dependent on the ability of Kindlin-1 to regulate integrin activity.

22

23

References

1. Driouch K, Bonin F, Sin S, *et al.* Confounding effects in "a six-gene signature predicting breast cancer lung metastasis": reply. *Cancer Res* 2009; 69: 9507-9511.

2. Landemaine T, Jackson A, Bellahcene A, *et al.* A six-gene signature predicting breast cancer lung metastasis. *Cancer Res* 2008; 68: 6092-6099.

3. Sin S, Bonin F, Petit V, *et al.* Role of the focal adhesion protein kindlin-1 in breast cancer growth and lung metastasis. *J Natl Cancer Inst* 2011; 103: 1323-1337.

4. Rognoni E, Ruppert R, Fassler R. The kindlin family: functions, signaling properties and implications for human disease. *J Cell Sci* 2016; 129: 17-27.

5. Has C, Castiglia D, del Rio M, *et al.* Kindler syndrome: extension of FERMT1 mutational spectrum and natural history. *Hum Mutat* 2011; 32: 1204-1212.

6. Lai-Cheong JE, Parsons M, Tanaka A, *et al.* Loss-of-function FERMT1 mutations in kindler syndrome implicate a role for fermitin family homolog-1 in integrin activation. *Am J Pathol* 2009; 175: 1431-1441.

7. Rognoni E, Widmaier M, Jakobson M, *et al.* Kindlin-1 controls Wnt and TGF-beta availability to regulate cutaneous stem cell proliferation. *Nat Med* 2014; 20: 350-359.

8. Patel H, Stavrou I, Shrestha RL, *et al.* Kindlin1 regulates microtubule function to ensure normal mitosis. *J Mol Cell Biol* 2016.

9. Patel H, Zich J, Serrels B, *et al.* Kindlin-1 regulates mitotic spindle formation by interacting with integrins and Plk-1. *Nat Commun* 2013; 4: 2056.

10. Andrechek ER, Hardy WR, Siegel PM, *et al.* Amplification of the neu/erbB-2 oncogene in a mouse model of mammary tumorigenesis. *Proc Natl Acad Sci U S A* 2000; 97: 3444-3449.

11. Guy CT, Cardiff RD, Muller WJ. Induction of mammary tumors by expression of polyomavirus middle T oncogene: a transgenic mouse model for metastatic disease. *Mol Cell Biol* 1992; 12: 954-961.

12. Ursini-Siegel J, Hardy WR, Zuo D, *et al.* ShcA signalling is essential for tumour progression in mouse models of human breast cancer. *EMBO J* 2008; 27: 910-920.

13. Luche H, Weber O, Nageswara Rao T, *et al.* Faithful activation of an extra-bright red fluorescent protein in "knock-in" Cre-reporter mice ideally suited for lineage tracing studies. *Eur J Immunol* 2007; 37: 43-53.

14.   Borowsky AD, Namba R, Young LJ, *et al.* Syngeneic mouse mammary carcinoma cell lines: two closely related cell lines with divergent metastatic behavior. *Clin Exp Metastasis* 2005; 22: 47-59.

15.   Qian B, Deng Y, Im JH, *et al.* A distinct macrophage population mediates metastatic breast cancer cell extravasation, establishment and growth. *PLoS One* 2009; 4: e6562.

16.   Lee S, Yoon IH, Yoon A, *et al.* An antibody to the sixth Ig-like domain of VCAM-1 inhibits leukocyte transendothelial migration without affecting adhesion. *J Immunol* 2012; 189: 4592-4601.

17.   Humphries JD, Byron A, Humphries MJ. Integrin ligands at a glance. *J Cell Sci* 2006; 119: 3901-3903.

18.   Moleirinho S, Chang N, Sims AH, *et al.* KIBRA exhibits MST-independent functional regulation of the Hippo signaling pathway in mammals. *Oncogene* 2013; 32: 1821-1830.

19.   Rajagopalan D. A comparison of statistical methods for analysis of high density oligonucleotide array data. *Bioinformatics* 2003; 19: 1469-1476.

20.   Pearce DA, Nirmal AJ, Freeman TC, Sims AH. Continuous biomarker assessment by exhaustive survival analysis. *bioRxiv* 2017; doi: 10.1101/208660.

21.   White DE, Kurpios NA, Zuo D, *et al.* Targeted disruption of beta1-integrin in a transgenic mouse model of human breast cancer reveals an essential role in mammary tumor induction. *Cancer Cell* 2004; 6: 159-170.

22.   Bazzoni G, Shih DT, Buck CA, *et al.* Monoclonal antibody 9EG7 defines a novel beta 1 integrin epitope induced by soluble ligand and manganese, but inhibited by calcium. *J Biol Chem* 1995; 270: 25570-25577.

23.   Harburger DS, Bouaouina M, Calderwood DA. Kindlin-1 and -2 directly bind the C-terminal region of beta integrin cytoplasmic tails and exert integrin-specific activation effects. *J Biol Chem* 2009; 284: 11485-11497.

24.   Ussar S, Moser M, Widmaier M, *et al.* Loss of Kindlin-1 causes skin atrophy and lethal neonatal intestinal epithelial dysfunction. *PLoS Genet* 2008; 4: e1000289.

25.   Labelle M, Hynes RO. The initial hours of metastasis: the importance of cooperative host-tumor cell interactions during hematogenous dissemination. *Cancer Discov* 2012; 2: 1091-1099.

26.   Wang H, Fu W, Im JH, *et al.* Tumor cell alpha3beta1 integrin and vascular laminin-5 mediate pulmonary arrest and metastasis. *J Cell Biol* 2004; 164: 935-941.

25

27.   Taichman DB, Cybulsky MI, Djaffar I, *et al.* Tumor cell surface alpha 4 beta 1 integrin mediates adhesion to vascular endothelium: demonstration of an interaction with the N-terminal domains of INCAM-110/VCAM-1. *Cell Regul* 1991; 2: 347-355.

28.   McAllister SS, Weinberg RA. The tumour-induced systemic environment as a critical regulator of cancer progression and metastasis. *Nat Cell Biol* 2014; 16: 717-727.

29.   Lowy CM, Oskarsson T. Tenascin C in metastasis: A view from the invasive front. *Cell Adh Migr* 2015; 9: 112-124.

30.   Patani N, Martin LA, Dowsett M. Biomarkers for the clinical management of breast cancer: international perspective. *Int J Cancer* 2013; 133: 1-13.

31.   Andres SA, Edwards AB, Wittliff JL. Expression of urokinase-type plasminogen activator (uPA), its receptor (uPAR), and inhibitor (PAI-1) in human breast carcinomas and their clinical relevance. *J Clin Lab Anal* 2012; 26: 93-103.

32.   Oskarsson T, Acharyya S, Zhang XH, *et al.* Breast cancer cells produce tenascin C as a metastatic niche component to colonize the lungs. *Nat Med* 2011; 17: 867-874.

33.   Minn AJ, Gupta GP, Siegel PM, *et al.* Genes that mediate breast cancer metastasis to lung. *Nature* 2005; 436: 518-524.

34.   Ferjancic S, Gil-Bernabe AM, Hill SA, *et al.* VCAM-1 and VAP-1 recruit myeloid cells that promote pulmonary metastasis in mice. *Blood* 2013; 121: 3289-3297.

35.   Qian BZ, Li J, Zhang H, *et al.* CCL2 recruits inflammatory monocytes to facilitate breast-tumour metastasis. *Nature* 2011; 475: 222-225.

36.   Bao L, Pigott R, Matsumura Y, *et al.* Correlation of VLA-4 integrin expression with metastatic potential in various human tumour cell lines. *Differentiation* 1993; 52: 239-246.

37.   Rebhun RB, Cheng H, Gershenwald JE, *et al.* Constitutive expression of the alpha4 integrin correlates with tumorigenicity and lymph node metastasis of the B16 murine melanoma. *Neoplasia* 2010; 12: 173-182.

38.   Garofalo A, Chirivi RG, Foglieni C, *et al.* Involvement of the very late antigen 4 integrin on melanoma in interleukin 1-augmented experimental metastases. *Cancer Res* 1995; 55: 414-419.

39.   Liang S, Dong C. Integrin VLA-4 enhances sialyl-Lewisx/a-negative melanoma adhesion to and extravasation through the endothelium under low flow conditions. *Am J Physiol Cell Physiol* 2008; 295: C701-707.

26

40. Klemke M, Weschenfelder T, Konstandin MH*, et al.* High affinity interaction of integrin alpha4beta1 (VLA-4) and vascular cell adhesion molecule 1 (VCAM-1) enhances migration of human melanoma cells across activated endothelial cell layers. *J Cell Physiol* 2007; 212: 368-374.

41. Okahara H, Yagita H, Miyake K*, et al.* Involvement of very late activation antigen 4 (VLA-4) and vascular cell adhesion molecule 1 (VCAM-1) in tumor necrosis factor alpha enhancement of experimental metastasis. *Cancer Res* 1994; 54: 3233-3236.

42. Soto MS, Serres S, Anthony DC*, et al.* Functional role of endothelial adhesion molecules in the early stages of brain metastasis. *Neuro Oncol* 2014; 16: 540-551.

43. Cardones AR, Murakami T, Hwang ST. CXCR4 enhances adhesion of B16 tumor cells to endothelial cells in vitro and in vivo via beta(1) integrin. *Cancer Res* 2003; 63: 6751-6757.

44. Huck L, Pontier SM, Zuo DM*, et al.* beta1-integrin is dispensable for the induction of ErbB2 mammary tumors but plays a critical role in the metastatic phase of tumor progression. *Proc Natl Acad Sci U S A* 2010; 107: 15559-15564.

45. Shibue T, Weinberg RA. Integrin beta1-focal adhesion kinase signaling directs the proliferation of metastatic cancer cells disseminated in the lungs. *Proc Natl Acad Sci U S A* 2009; 106: 10290-10295.

46. Takenaka K, Shibuya M, Takeda Y*, et al.* Altered expression and function of beta1 integrins in a highly metastatic human lung adenocarcinoma cell line. *Int J Oncol* 2000; 17: 1187-1194.

47. Barkan D, Kleinman H, Simmons JL*, et al.* Inhibition of metastatic outgrowth from single dormant tumor cells by targeting the cytoskeleton. *Cancer Res* 2008; 68: 6241-6250.

48. Shibue T, Brooks MW, Inan MF*, et al.* The outgrowth of micrometastases is enabled by the formation of filopodium-like protrusions. *Cancer Discov* 2012; 2: 706-721.

Figure 1. Kindlin-1 loss delays tumor onset but not growth of established tumors.
(A) Kaplan–Meier analysis of tumor onset in MT-Kin-1$^{fl/fl}$ (n = 16) and MT-Kin-1$^{wt/wt}$ (n = 10) mice (P < 0.0001, log-rank test). (B) Quantification of area covered by focal lesions in mammary glands from MT-Kin-1$^{fl/fl}$ and MT-Kin-1$^{wt/wt}$ mice. Values are means $\pm$ SEM (n = 4 mice; **P < 0.01). (C) Representative H&E staining of fat pads from 28-day-old MT-Kin-1$^{fl/fl}$ and MT-Kin-1$^{wt/wt}$ mice. Scale bar, 50 μm. (D) Box-and-whisker plots of tumor doubling times in MT-Kin-1$^{fl/fl}$ and MT-Kin-1$^{wt/wt}$ mice (n = 6 mice; non-significant, P = 0.1797). (E) Quantification of percentage of Ki67-positive (Ki67+) cells within size-matched tumors from MT-Kin-1$^{fl/fl}$ and MT-Kin-1$^{wt/wt}$ mice. Values are means $\pm$ SEM (n = 4 mice; non-significant, P = 0.0812). (F) Representative H&E staining of tumors from MT-Kin-1$^{fl/fl}$ and MT-Kin-1$^{wt/wt}$ mice. Scale bar, 50 μm.

Figure 2. Kindlin-1 loss reduces pulmonary metastasis. (A) Incidence of metastatic lesions in the lungs of MT-Kin-1$^{fl/fl}$ (n = 16) or MT-Kin-1$^{wt/wt}$ (n = 10) mice. (B) Representative H&E staining of lung metastases in MT-Kin-1$^{fl/fl}$ and MT-Kin-1$^{wt/wt}$ mice. Scale bar, 50 μm. (C) PCR analysis of PyV MT in lungs from MT-Kin-1$^{fl/fl}$ or MT-Kin-1$^{wt/wt}$ mice normalized to the total primary tumor burden in each mouse. Values are means $\pm$ SEM (n = 7 mice; *P < 0.05, Student's t-test). (D) Box-and-whisker plots of lung weights collected 8 weeks after injection of dissociated tumors from MT-Kin-1$^{fl/fl}$ or MT-Kin-1$^{wt/wt}$ mice (n = 20 mice; **P < 0.01, Student's t-test). (E) Box-and-whisker plots of total area covered by metastatic lesions in lungs after injection of dissociated tumors from MT-Kin-1$^{fl/fl}$ or MT-Kin-1$^{wt/wt}$ mice (n = 20 mice; **P < 0.01, Student's t-test). (F) Quantification of number of metastatic nodules per lung. Each point represents an individual mouse (n = 17 mice; non-

28

significant, $P = 0.1329$). (G) Quantification of the size of individual metastatic nodules per lung. Each point represents an individual metastatic nodule ($n = 7$ mice; ****$P < 0.0001$, Student's t-test). (H) Quantification of percentage of Ki67-positive cells in lung metastases ($n = 7$ mice; non-significant, $P = 0.1192$).

Figure 3. Kindlin-1 regulates integrin activation and metastatic colonization. (A, B) Expression of active β1 integrin (A) and total β1 integrin (B) expression assessed by flow cytometry in mammary tumors from MT-Kin-1$^{fl/fl}$ and MT-Kin-1$^{wt/wt}$ mice. Values are means $\pm$ SEM ($n = 3$ mice; *$P < 0.05$, Student's t-test). (C) Western blot analysis demonstrating the re-expression of His-tagged Kindlin-1-WT or Kindlin-1-AA into Kindlin-1-Null A1 cells. Actin was used as a loading control. (D) Ratio of active β1 integrin to total β1 integrin expression. Values are normalized to WT cells and are means $\pm$ SEM ($n = 4$; **$P < 0.01$, ***$P < 0.001$, one-way ANOVA with Tukey's *post hoc* correction). (E) Adhesion to fibronectin expressed as number of adherent cells relative to WT cells. Values are means $\pm$ SEM ($n = 3$; **$P < 0.01$, one-way ANOVA with Tukey's *post hoc* correction). (F) PCR analysis of PyV MT in lungs 21 days post-injection of A1 Null, WT or AA cells. Values are normalized to WT cells and are means $\pm$ SEM ($n = 6$ mice; ****$P < 0.0001$, one-way ANOVA with Tukey's *post hoc* correction). (G) PCR analysis of PyV MT in lungs 30 minutes post-injection of A1 Null, WT or AA cells. Values are normalized to WT cells and are means $\pm$ SEM ($n = 6$ mice; **$P < 0.01$, ***$P < 0.001$, one-way ANOVA with Tukey's *post hoc* correction).

Figure 4. Kindlin-1 regulates cellular adhesion to endothelial cells and pulmonary arrest in an integrin-dependent manner. (A) Adhesion to VCAM-1 in

29

the presence of function-blocking anti-α4 integrin antibody or isotype IgG control expressed as number of adherent cells relative to WT. Values are means $\pm$ SEM ($n = 3$; ****$P < 0.0001$). (B) Adhesion to endothelial cells expressed as number of adherent cells relative to WT cells. Values are means $\pm$ SEM ($n = 3$; ***$P < 0.001$). (C) Adhesion to endothelial cells in the presence of function-blocking anti-VCAM-1 antibody or isotype IgG control expressed as number of adherent cells relative to WT. Values are means $\pm$ SEM ($n = 3$; **$P < 0.01$, ***$P < 0.001$). (D) PCR analysis of PyV MT in lungs 30 minutes post-injection of A1 Null, WT or AA cells in the presence of function-blocking anti-VCAM-1 antibody or isotype IgG control. Values are means $\pm$ SEM ($n = 4$ mice; **$P < 0.01$, two-way ANOVA with Bonferroni's *post hoc* correction). (E) PCR analysis of PyV MT in lungs 30 minutes post-injection of A1 WT in the presence of function-blocking anti-α4 integrin antibody or isotype IgG control. Values are means $\pm$ SEM ($n = 12$ mice; **$P < 0.01$, Student's *t*-test).

Figure 5. Kindlin-1 regulates the mammary tumor cell secretome. (A) Gene ontology enrichment analysis of top-level cellular component terms significantly overrepresented in the proteomic dataset of the A1 Null and WT secretomes ($P < 0.001$, hypergeometric test with Benjamini–Hochberg *post hoc* correction). (B) Hierarchically clustered heatmap of median-centered, normalized protein intensities quantified by label-free MS. Significantly differentially regulated extracellular proteins are shown (FDR = 5%, Student's *t*-test). Gray bars indicate reported associations with tumor metastasis; adjacent colored bars (Met. regul[n]) indicate reported up-regulation (red), down-regulation (blue) or both (gray) in metastasis signatures. (C) Functional enrichment analysis of the significantly differentially regulated extracellular proteins in (B). Parent or sibling overrepresented functions are

30

grouped together and displayed as a heatmap (log_{10} color scale) ($P < 0.05$, hypergeometric test with Benjamini–Hochberg *post hoc* correction). (D) Volcano plot of extracellular proteins quantified in the A1 Null and WT secretomes. Black curves show the threshold for significant differential regulation (FDR = 5%, Student's *t*-test). Proteins differentially regulated by more than 16-fold ($P < 0.001$) are labeled. (E) Topological analysis of the Kindlin-1-dependent Met-1 secretome network (see Supplementary Fig. S6). Clustering coefficient represents the capacity for groups of proteins to be connected. Proteins with a clustering coefficient greater than 0.35 are labeled. (F) Integrative network analysis of the Kindlin-1-dependent secretome directly associated with PAI-1 and tenascin-C. Protein node (circle) size is proportional to FDR-adjusted *P* of differential regulation (*Q*); node color represents log_2-transformed fold change. Connecting edge (line) color represents relationship type; edge thickness is proportional to a linear regression–derived network weighting. The graph was clustered using a force-directed algorithm.

Figure 6. Kindlin-1 dependent secretome is associated with lung metastasis and is elevated in cells metastatic to lung. (A) PCR analysis of *Tnc* and *Serpine1* in A1 Null, WT or AA cells. Expression values are normalized to WT cells and are means $\pm$ SEM ($n = 4$; **$P < 0.01$, one-way ANOVA with Tukey's *post hoc* correction). (B) MDA-MB-231 subpopulations with enhanced lung metastatic activity have elevated expression of *FERMT1* and *TNC*. (C) Comparison of expression of *FERMT1, TNC* and *SERPINE1* in MDA-MB-231 subpopulations predisposed or not predisposed to lung metastasis (*$P = 0.05$, **$P = 0.008$, ***$P = 0.001$, Wilcoxon test). (D) Comparison of expression of *FERMT1*, *TNC* and *SERPINE1* in 2999 primary breast tumors split into those where *FERMT1* expression is detected (***$P < 0.001$,

31

Wilcoxon test). (E) Cox proportional hazards survival analysis of the Kindlin-1-dependent secretome genes represented in a primary breast cancer dataset (MSK82, GSE2603; $n = 82$). Patients were stratified at all possible cut-points for all secretome genes, and the proportions of cut-points significantly associated with lung (green bars) and non-lung (gray diamonds) metastasis ($P < 0.05$) are shown for each gene. For clarity, genes not significantly associated with lung metastasis at any cut-point ($P \geq 0.05$) are not displayed. The secretome genes were significantly more associated with worse outcomes in terms of lung metastasis as compared to non-lung metastasis (****$P = 3.96 \times 10^{-5}$, Wilcoxon test).
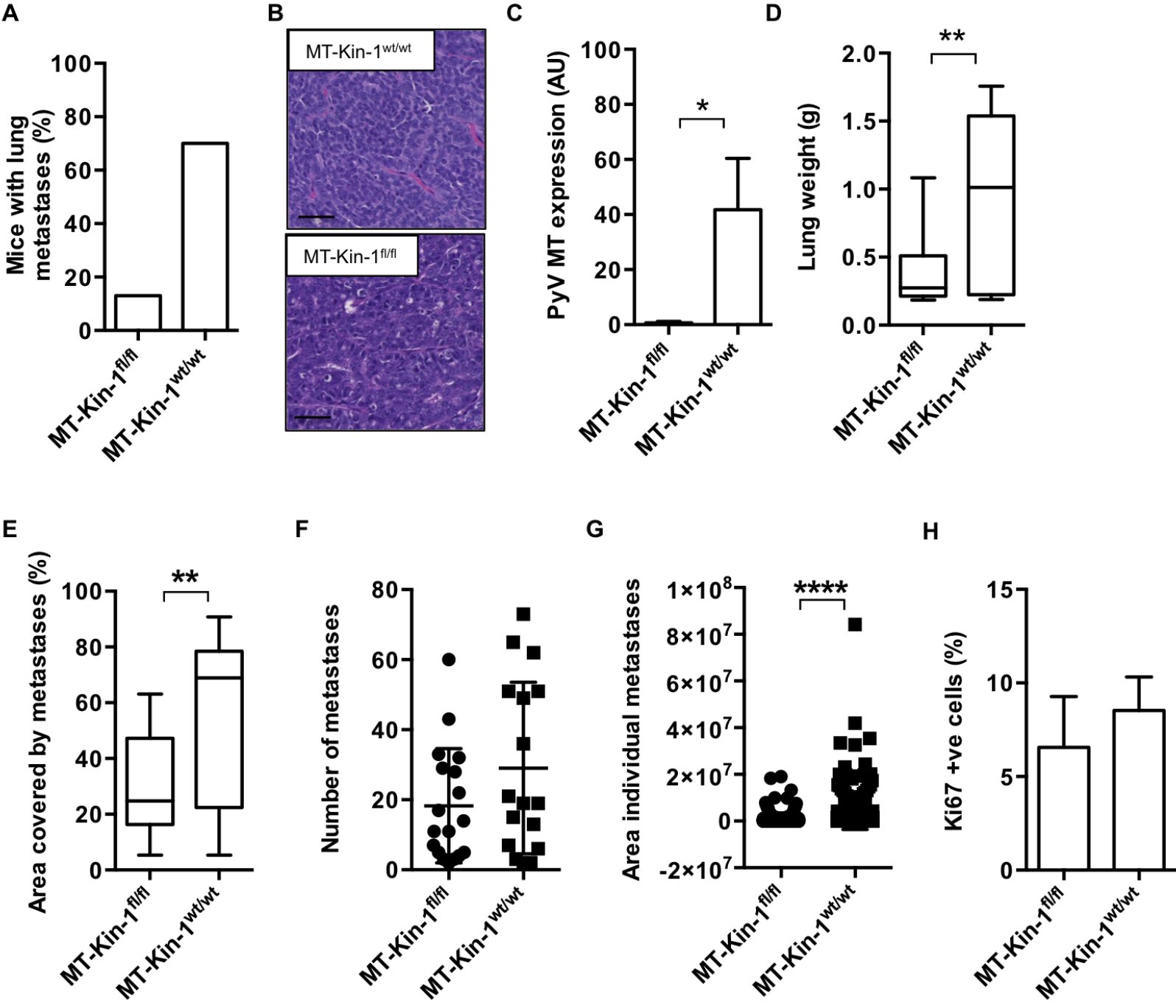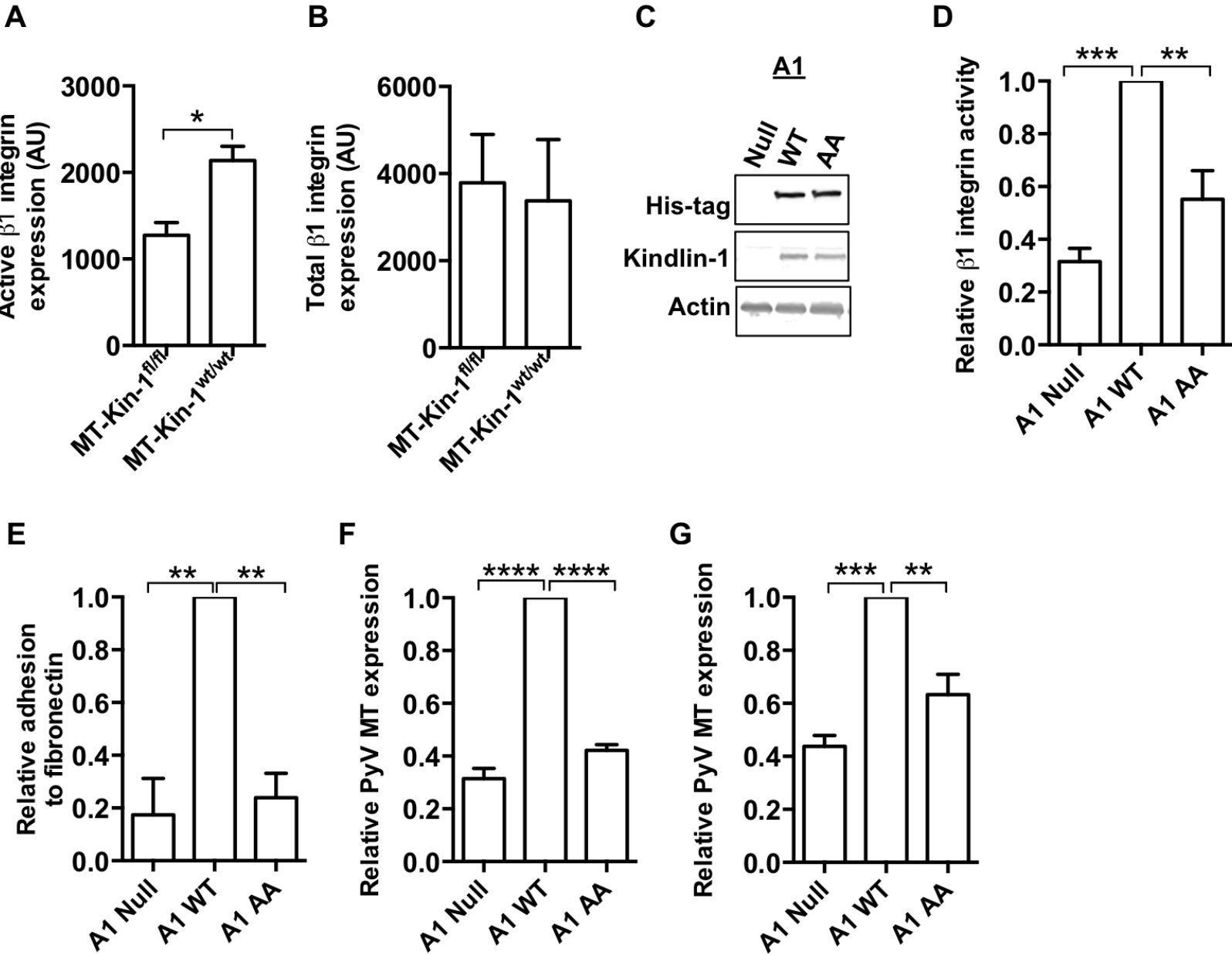
Figure 1
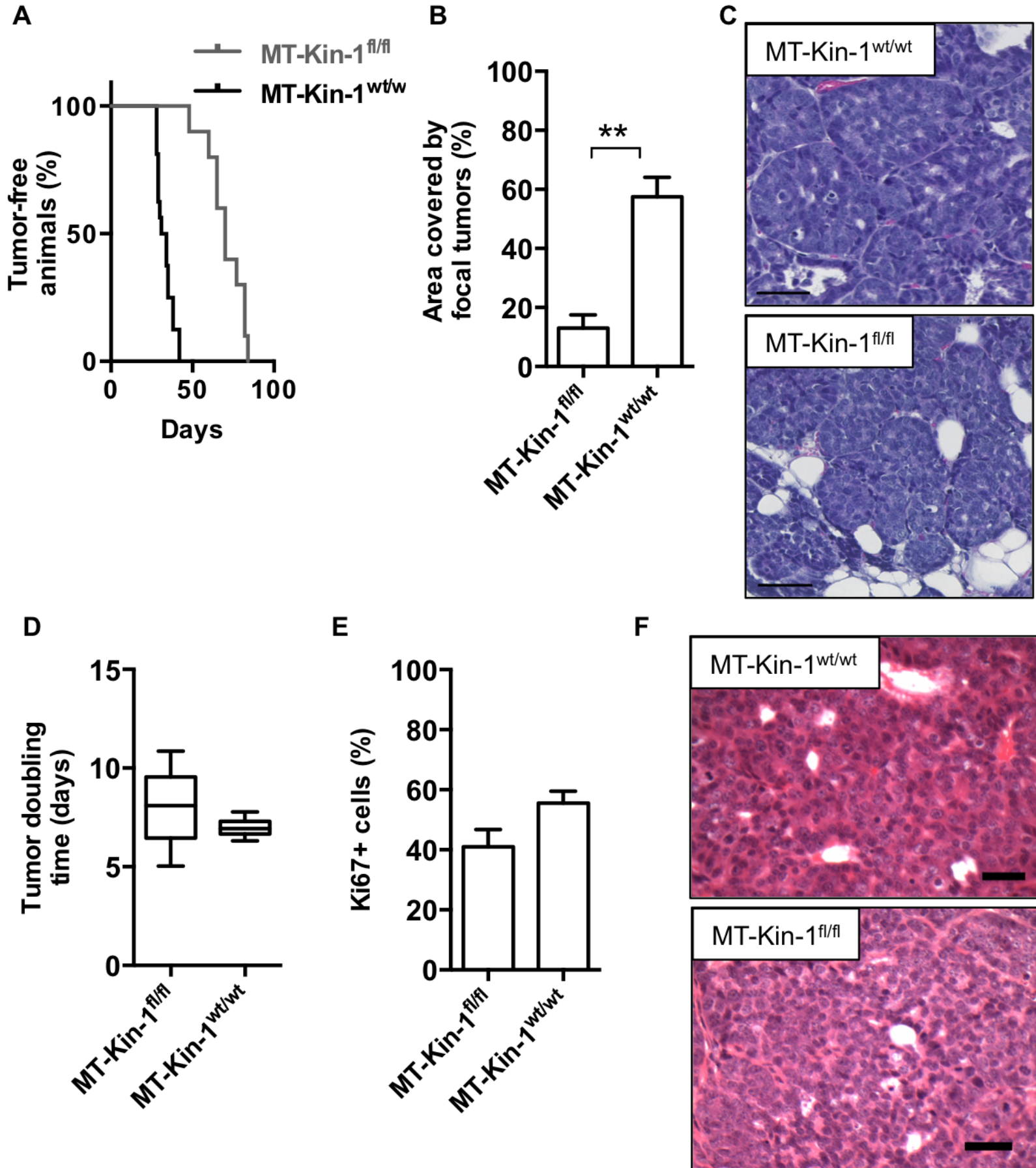
Figure 2

Figure 3

Figure 4

Figure 5
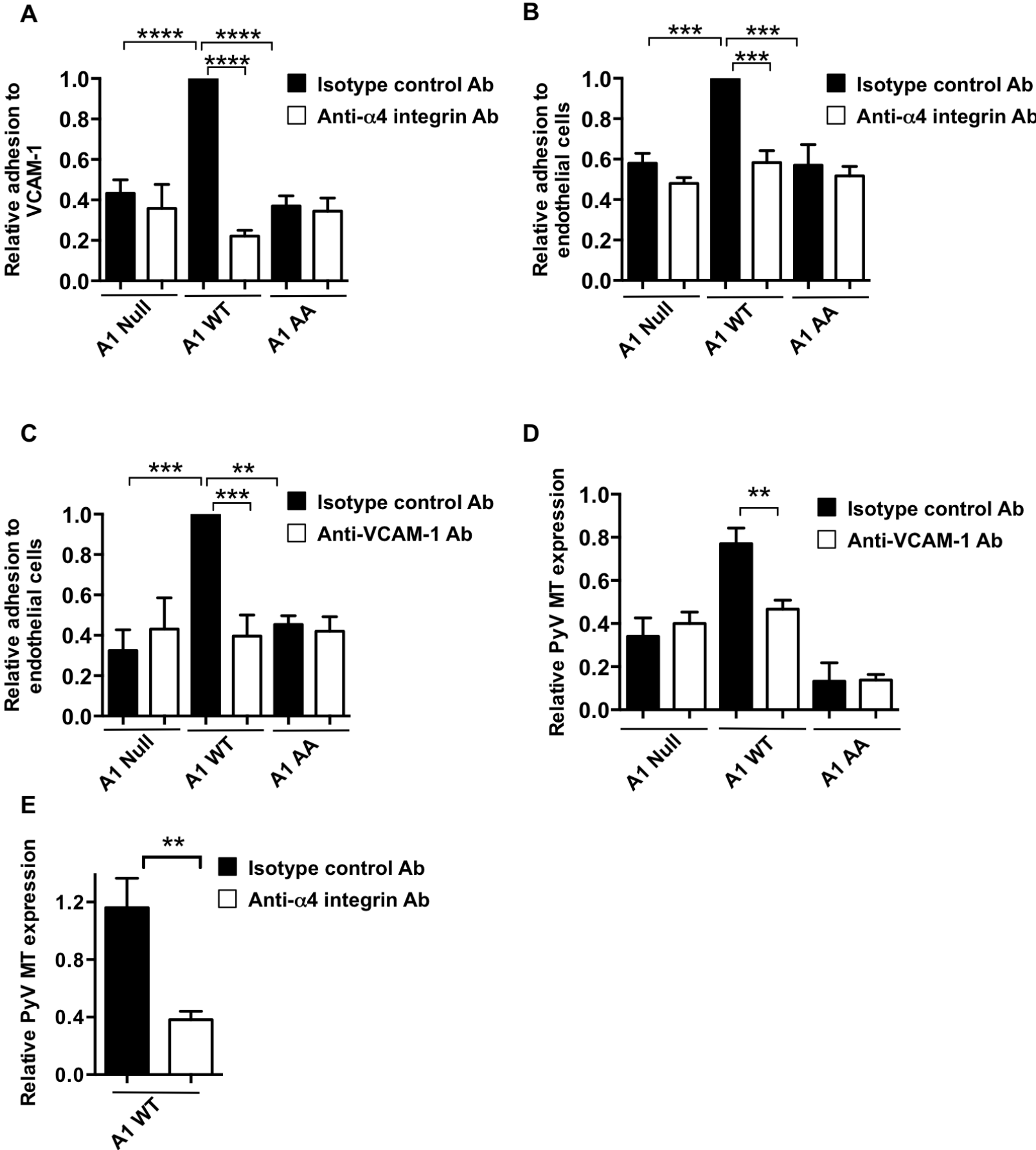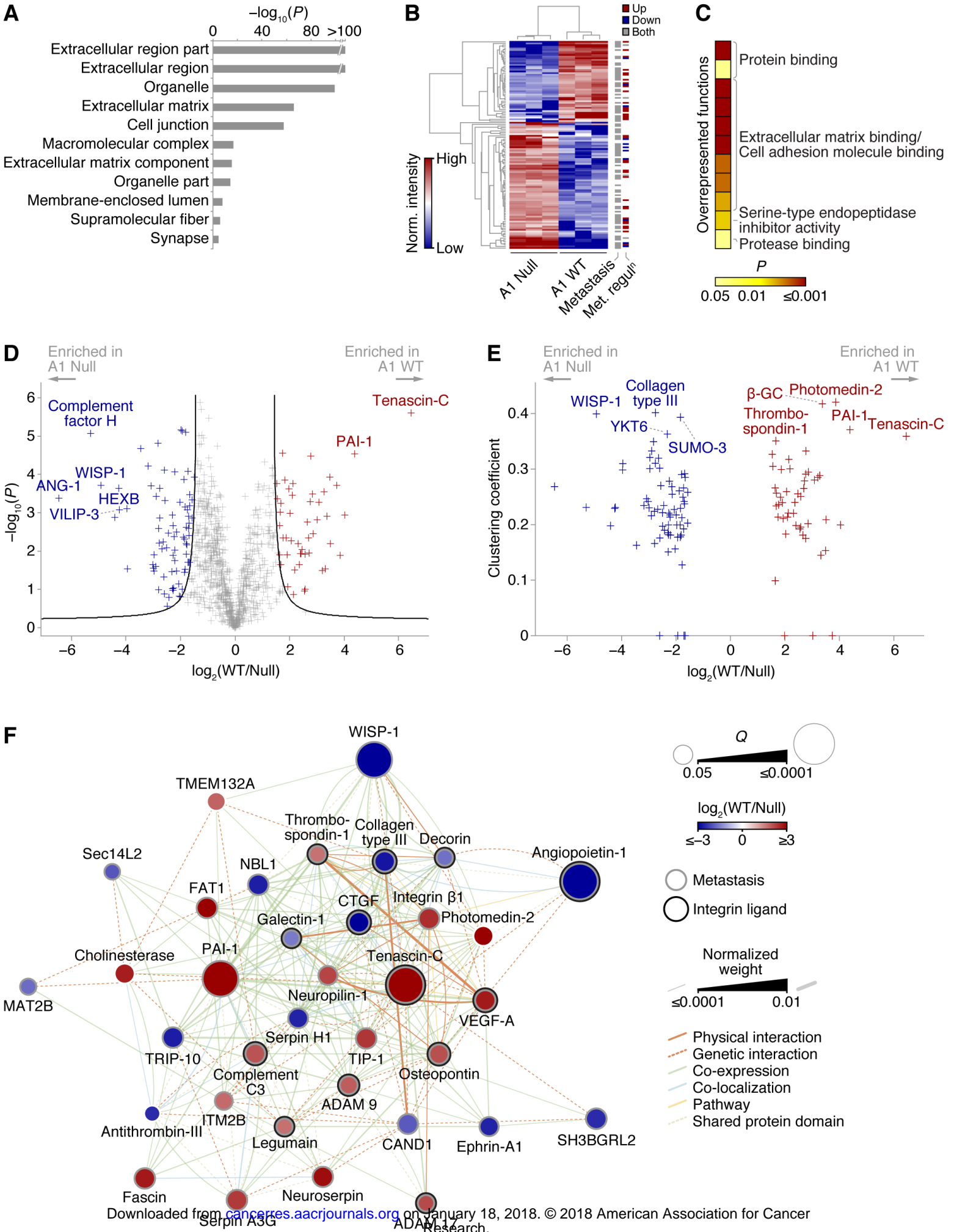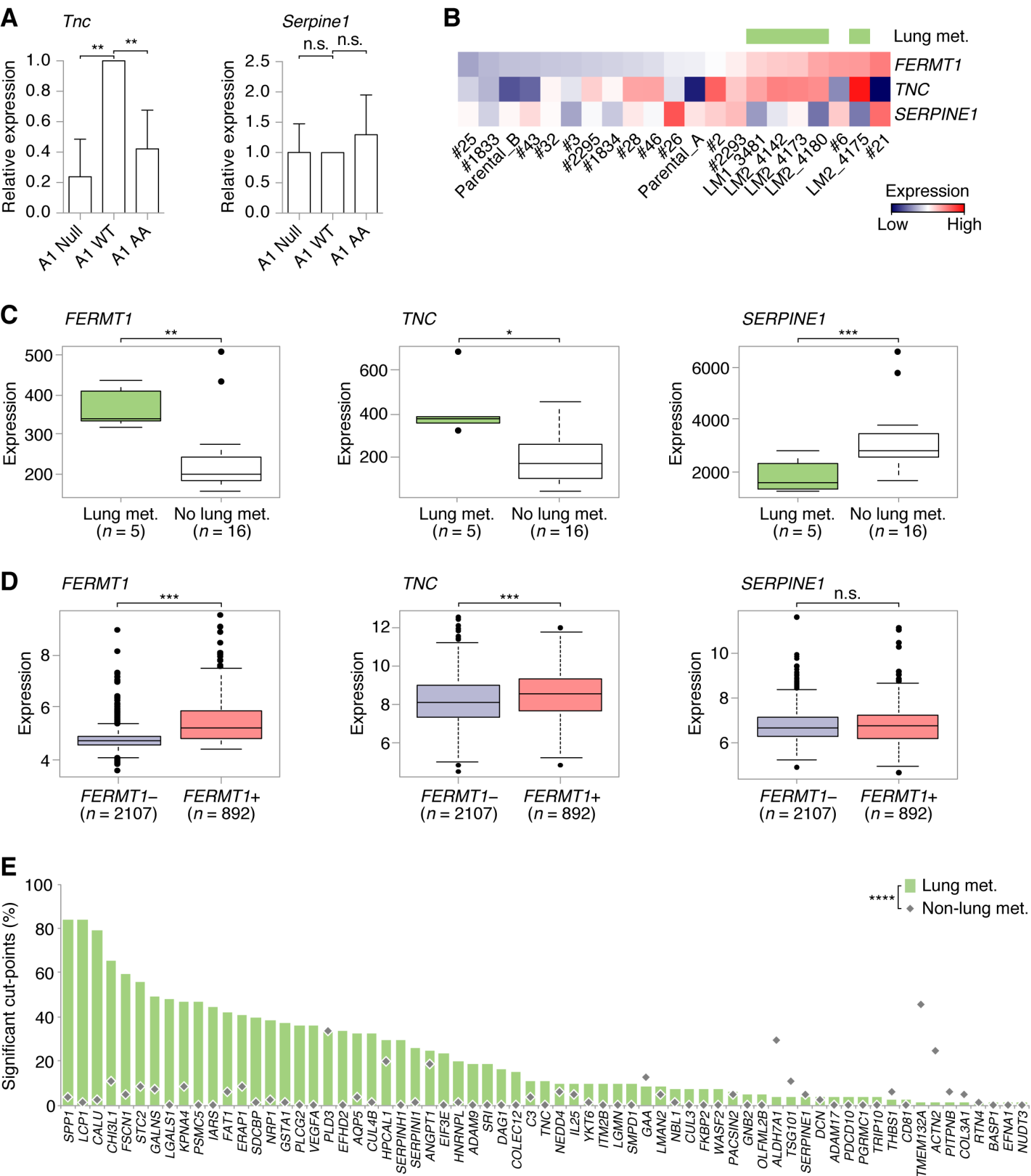
Figure 6

AAC-R American Association for Cancer Research

Cancer Research

The Journal of Cancer Research (1916–1930) | The American Journal of Cancer (1931–1940)

Kindlin-1 promotes pulmonary breast cancer metastasis

Sana Sarvi, Hitesh Patel, Jun Li, et al.

Updated version	Access the most recent version of this article at: doi:10.1158/0008-5472.CAN-17-1518
Supplementary Material	Access the most recent supplemental material at: http://cancerres.aacrjournals.org/content/suppl/2018/01/12/0008-5472.CAN-17-1518.DC1
Author Manuscript	Author manuscripts have been peer reviewed and accepted for publication but have not yet been edited.

E-mail alerts	Sign up to receive free email-alerts related to this article or journal.
Reprints and Subscriptions	To order reprints of this article or to subscribe to the journal, contact the AACR Publications Department at pubs@aacr.org.
Permissions	To request permission to re-use all or part of this article, use this link http://cancerres.aacrjournals.org/content/early/2018/01/12/0008-5472.CAN-17-1518. Click on "Request Permissions" which will take you to the Copyright Clearance Center's (CCC) Rightslink site.